

Supporting Information

Contact Properties at the Metal–MoS₂/WSe₂ Hetero-bilayer

Interfaces

Dongqing Zou¹, Wenkai Zhao ^{*1}, Yuqing Xu¹, Xiaoteng Li¹, Yuliang Liu¹ and
Chuanlu Yang^{*1}

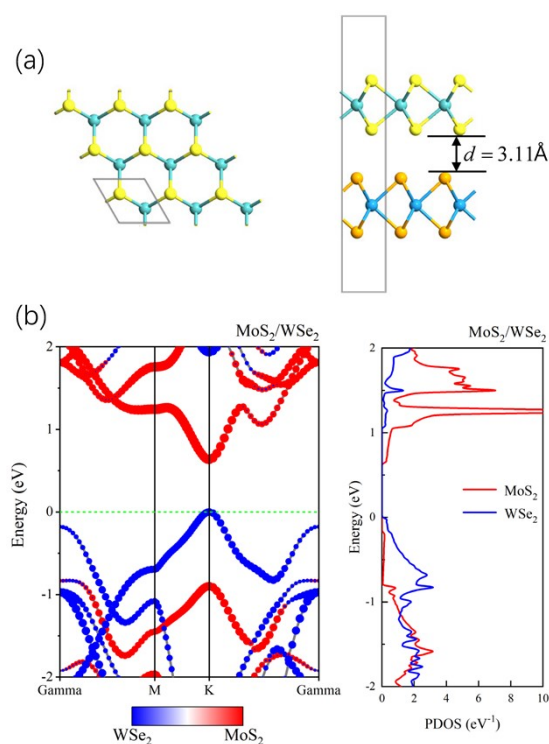


Fig. S1. (a) Top and side views of MoS₂/WSe₂ hetero-bilayer. The gray line marks the unit cell. The interlayer distance d is indicated by black arrow. (b) Projected band structure and projected density of states (PDOS) of MoS₂/WSe₂ hetero-bilayer. The Fermi level is set to zero.

¹ School of Physics and Optoelectronics Engineering, Ludong University, Yantai, 264025, People's Republic of China.

* E-mail: ycl@ldu.edu.cn, kaypu@ldu.edu.cn

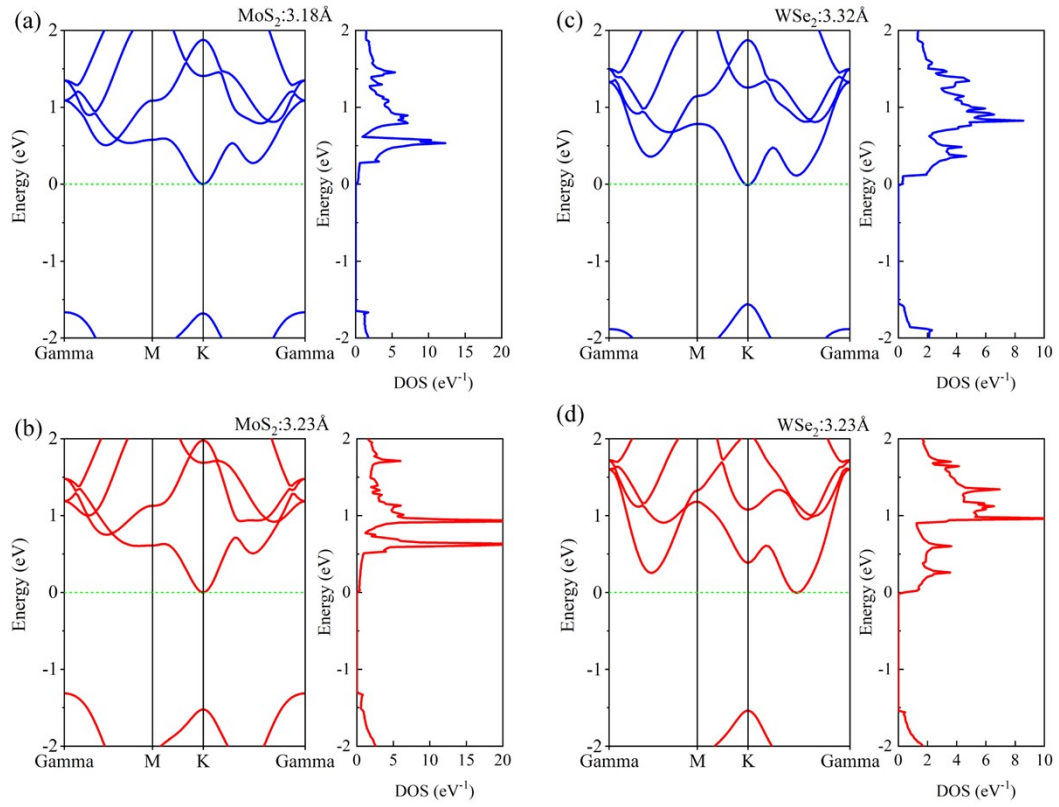


Fig. S2. Band structure and density of states (DOS) of MoS₂ or WSe₂ before and after strain. The blue line represents the situation before strain, and the red line represents the situation after strain. The Fermi level is set to zero.

We compare the effects of metal introduction on the band structure of MoS₂/WSe₂ hetero-bilayers before and after. For metals Al, Ag, Au, Pd, and Pt, which are 2×2 metal-matched with $\sqrt{3} \times \sqrt{3}$ MoS₂/WSe₂ vdWHs, we have compared the effect of stress changes in the $\sqrt{3} \times \sqrt{3}$ MoS₂/WSe₂ supercell lattice before and after the introduction of different metals on the band structure, as shown in Fig. S3(a). We found that the overall shape of the band structure is almost unaffected, but it mainly affects the position of the valence band maximum (VBM). For Al, the supercell lattice remains unchanged before and after introducing Al, and the band structure remains almost the same. For the other four metals, the position of the VBM at the gamma point is changed. The introduction of Ag and Au results in supercell lattice stretching, with strains of 1.61% and 0.89%, respectively. In the projected band diagram, the VBM of both MoS₂ and WSe₂ has shifted upward. The introduction of Pt and Pd metals may result in supercell lattice compression, with strains of 1.25%. The VBM of both MoS₂ and WSe₂ has shifted downward. For the metal Ti, it is a 1×1 metal-matched 1×1 MoS₂/WSe₂ vdWH. We also compared the effect of lattice strain on the band structure before and after the introduction of Ti. The lattice constant is compressed from 3.26Å to 3.09Å, with a strain of 5.2%. Due to the significant lattice change, both the shape and position of the band structure are noticeably affected, as shown in Fig. S3(b).

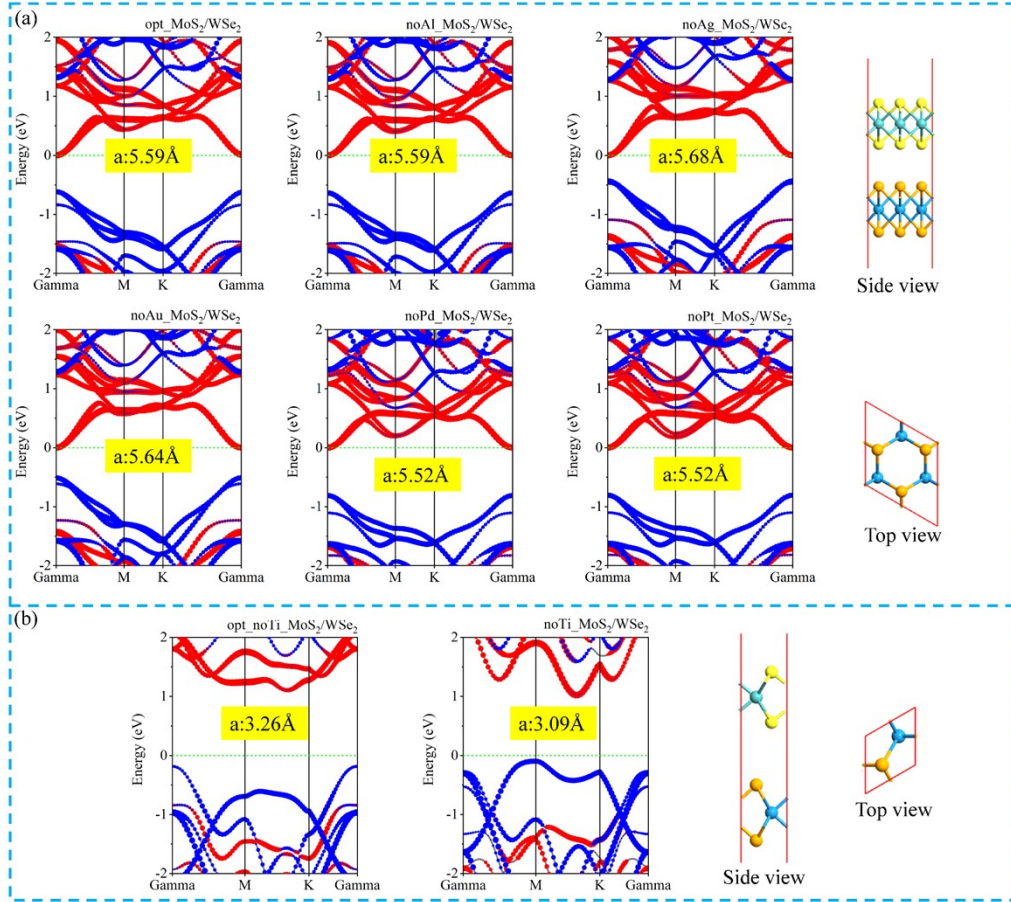


Fig. S3. Projected band structure and optimized geometry of (a) $\sqrt{3} \times \sqrt{3}$ MoS₂/WSe₂ vdWHs and (b) 1×1 MoS₂/WSe₂ vdWHs before and after strain. In the band diagram, the red line represents MoS₂, and the blue line represents WSe₂. The lattice constant "a" of the corresponding systems are displayed in the yellow box. The Fermi level is set to zero.

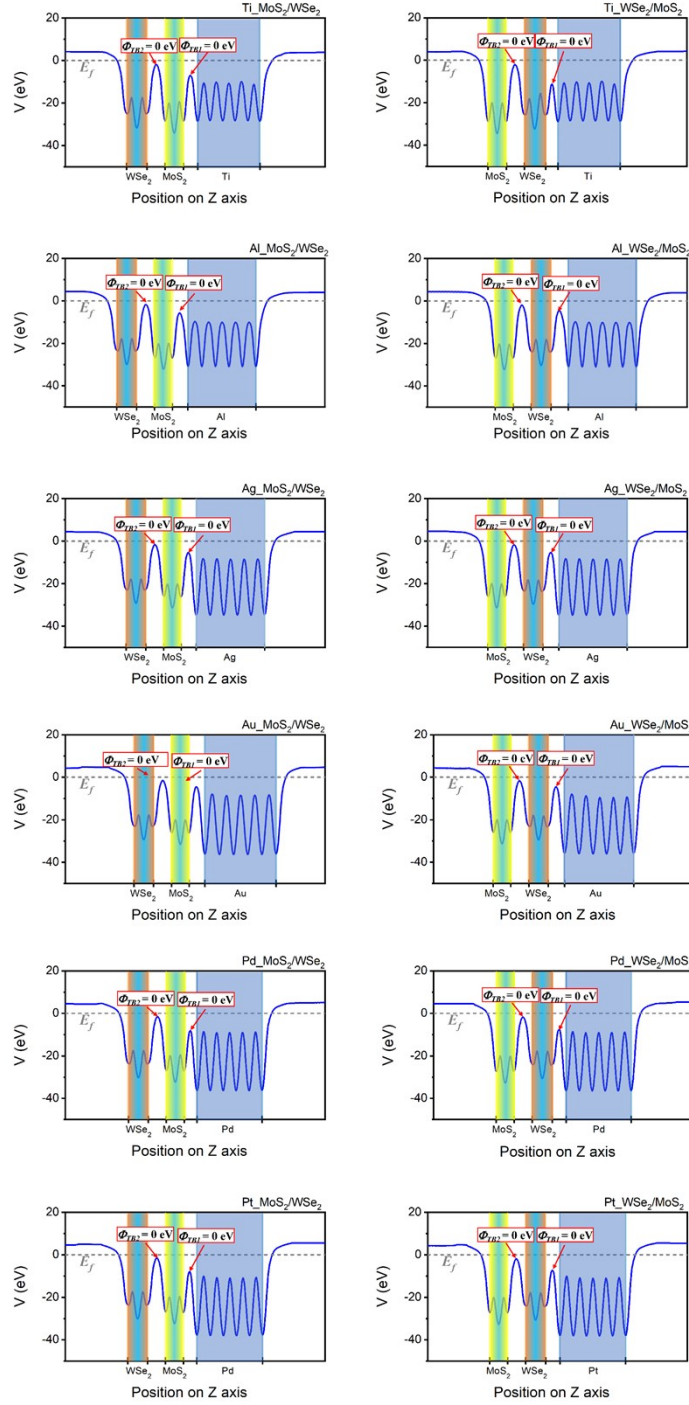


Fig. S4. Average electrostatics potential V versus position Z for the metal_ MoS_2 / WSe_2 hetero-bilayer contact along the vertical Z -direction normal to the interface. The left column of the picture illustrates the different metals contact next to MoS_2 layer and the right one shows next to WSe_2 layer. Different color areas represent the locations of different atoms. The carriers are injected from metal layer to MoS_2 and WSe_2 layer. Gray dash lines denote the Fermi level (E_f) which are set to zero.

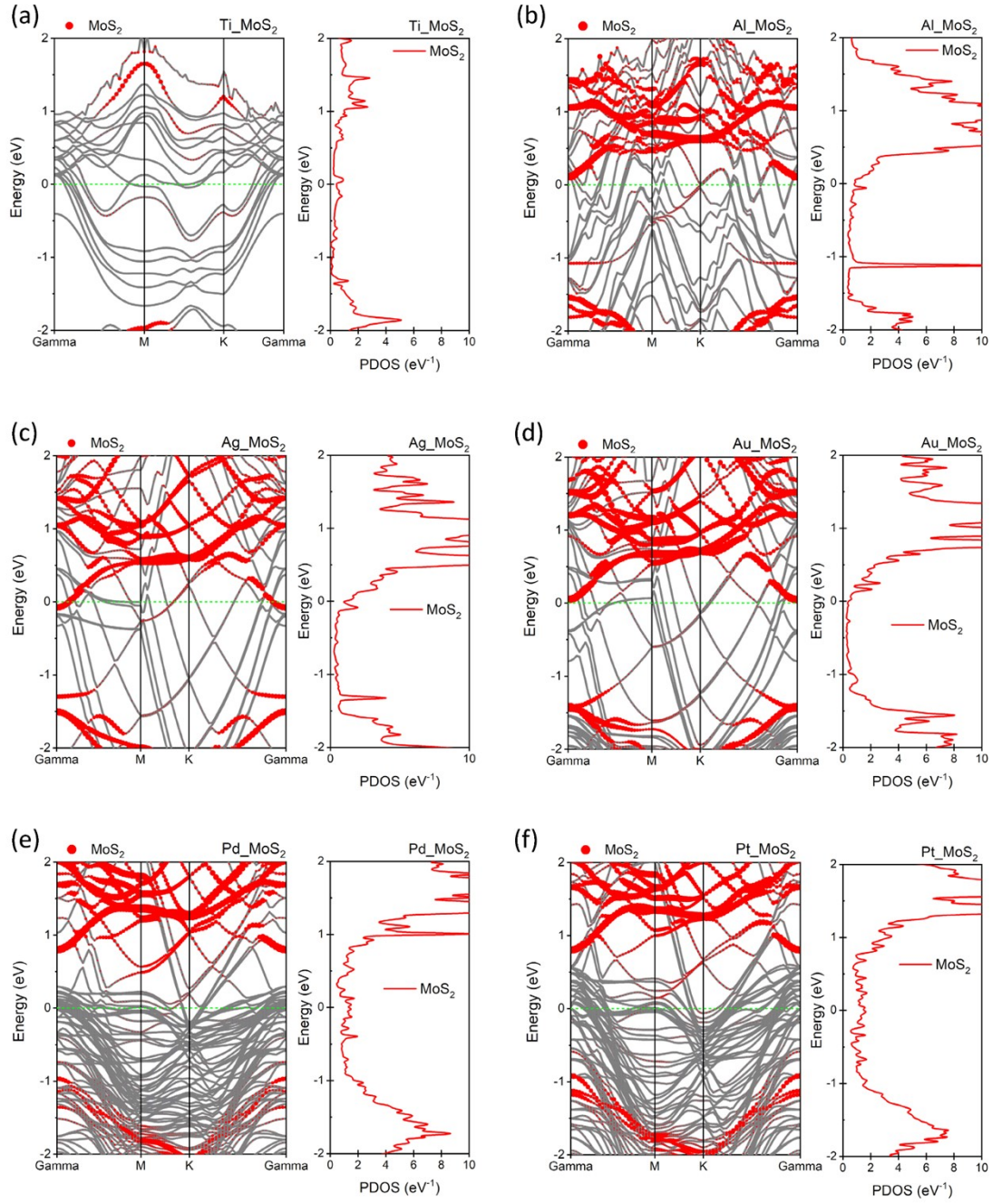


Fig. S5. Projected band structures (left column) and projected density of states (PDOS, right column) of (a) Ti_MoS₂, (b) Al_MoS₂, (c) Ag_MoS₂, (d) Au_MoS₂, (e) Pd_MoS₂, (f) Pt_MoS₂. The red represents the projected band structures and PDOS of MoS₂, and the gray curves represent band structures of the whole heterostructures. The Fermi level is set to zero.

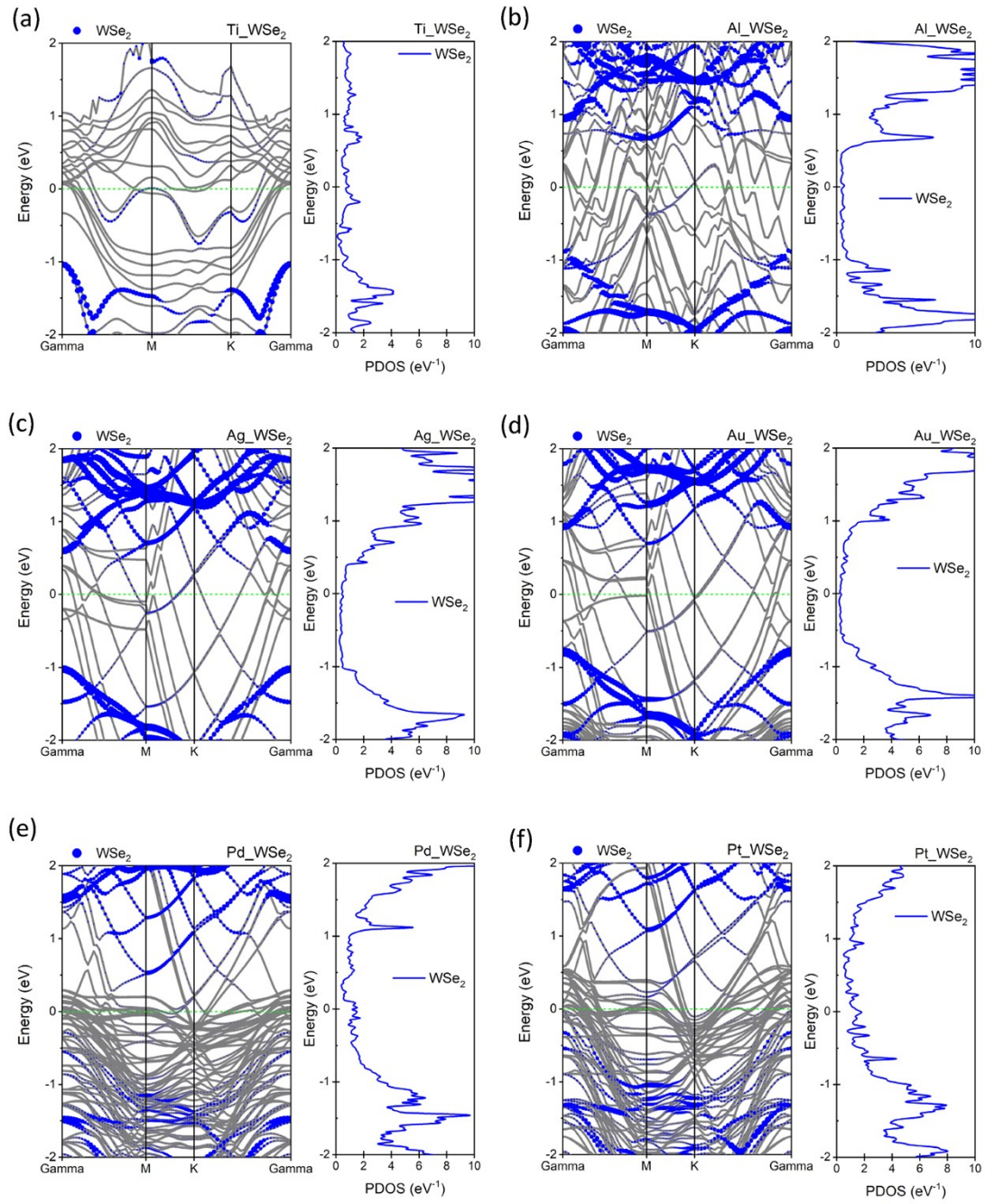


Fig. S6. Band structures and PDOS of (a) Ti_WSe₂, (b) Al_WSe₂, (c) Ag_WSe₂, (d) Au_WSe₂, (e) Pd_WSe₂, (f) Pt_WSe₂. The blue represents the projected band structures and PDOS of WSe₂, and the gray curves represent band structures of the whole heterostructures. The Fermi level is set to zero.

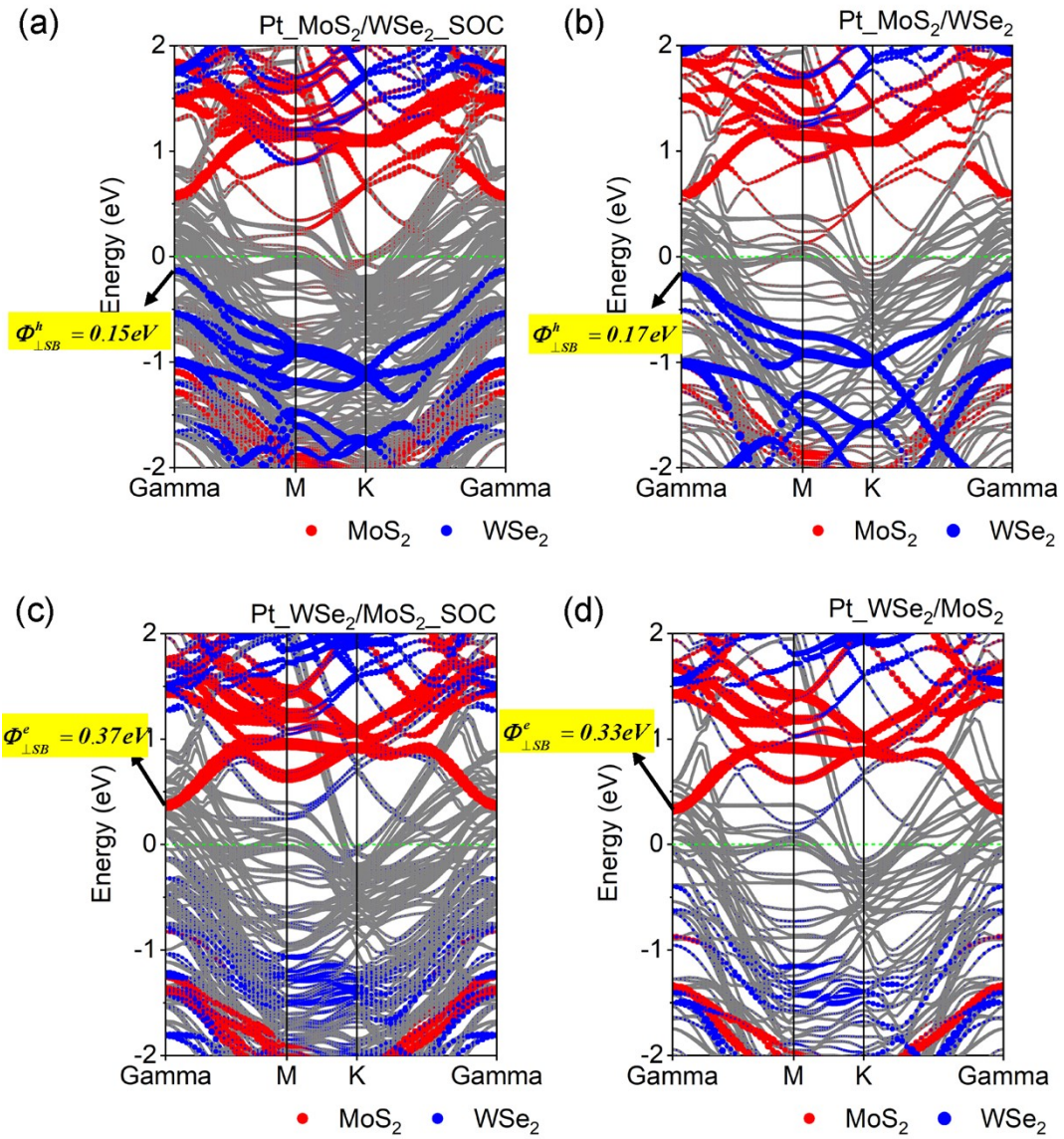


Fig. S7. Projected band structures of (a) Pt_MoS₂/WSe₂ with SOC, (b) Pt_MoS₂/WSe₂ without SOC, (c) Pt_WSe₂/MoS₂ with SOC and (d) Pt_WSe₂/MoS₂ without SOC.

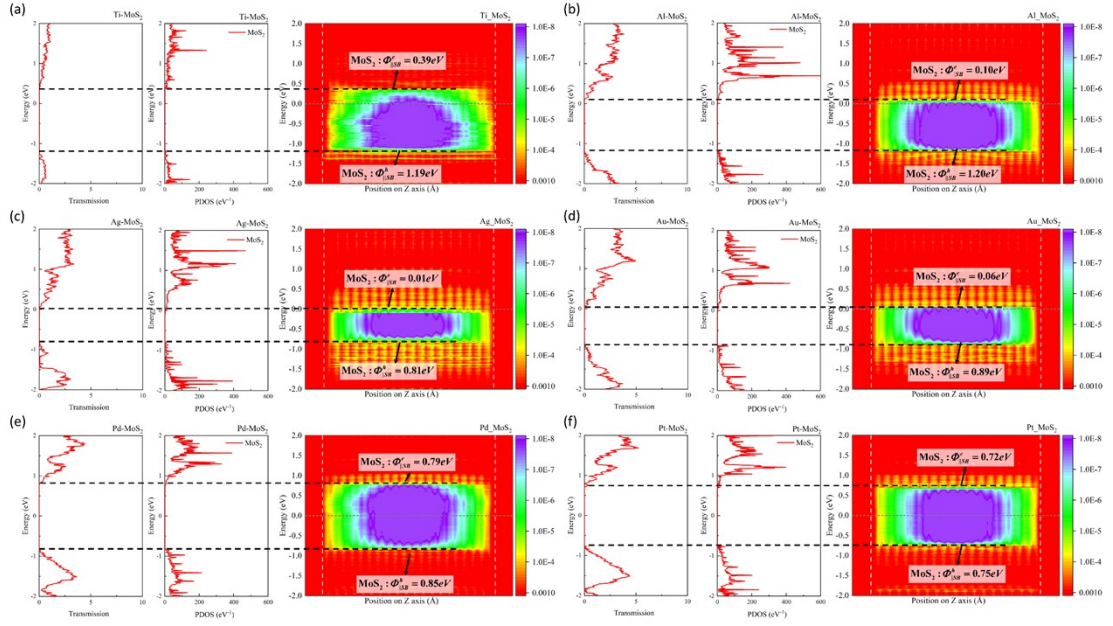


Fig. S8. total transmission (left column), PDOS projected on MoS₂ (middle column), LDDOS (right column) of (a) Ti_MoS₂, (b) Al_MoS₂, (c) Ag_MoS₂, (d) Au_MoS₂, (e) Pd_MoS₂, (f) Pt_MoS₂ under zero bias. Φ_{PSB}^e and Φ_{PSB}^h shows the SBHs of electrons and holes in the lateral direction marked with horizontal black dotted lines. The vertical white dotted lines are the boundaries between the electrode and channel regions.

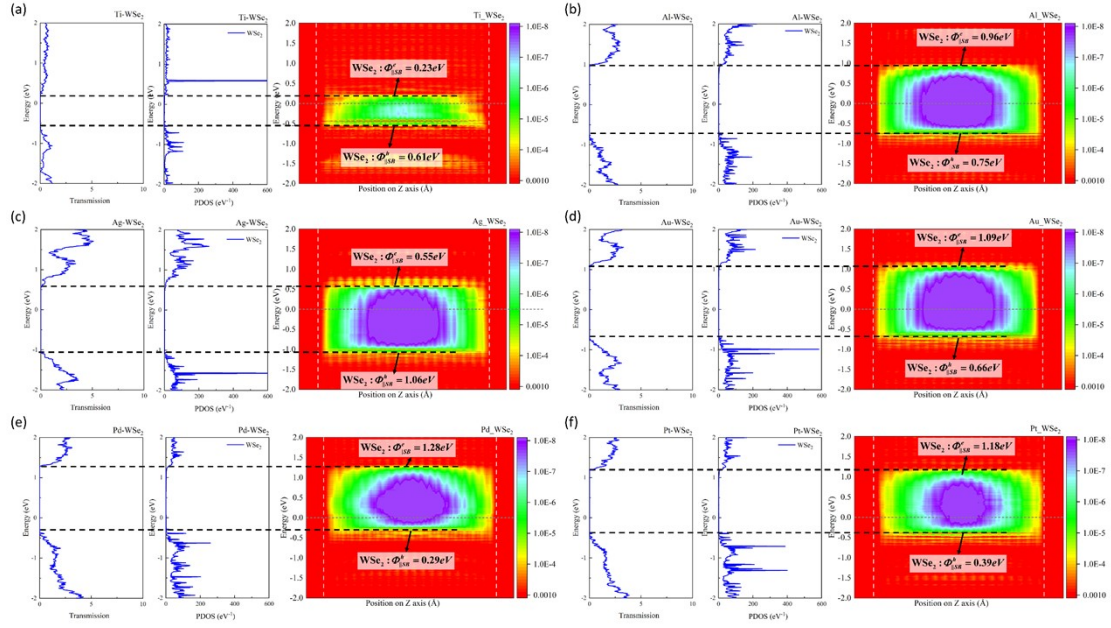


Fig. S9. total transmission (left column), PDOS projected on WSe₂ (middle column), LDDOS (right column) of (a) Ti_WSe₂, (b) Al_WSe₂, (c) Ag_WSe₂, (d) Au_WSe₂, (e) Pd_WSe₂, (f) Pt_WSe₂ under zero bias. Φ_{PSB}^e and Φ_{PSB}^h shows the SBHs of electrons and holes in the lateral direction marked with horizontal black dotted lines. The vertical white dotted lines are the boundaries between the electrode and channel regions.